


Theory of multiqubit superradiance in a waveguide in the presence of finite delay times and two quantum excitations

Sofia Arranz Regidor¹, Franco Nori^{2,3}, and Stephen Hughes¹

¹*Department of Physics, Engineering Physics and Astronomy, Queen's University, Kingston, Ontario, Canada K7L 3N6*

²*Quantum Computing Center, RIKEN, Wakoshi, Saitama 351-0198, Japan*

³*Department of Physics, University of Michigan, Ann Arbor, Michigan 48109-1040, USA*

 (Received 23 June 2025; revised 26 August 2025; accepted 27 October 2025; published 1 December 2025)

We study the quantum nonlinear dynamics of multiple two-level atoms (qubits) in a waveguide quantum electrodynamics system, with a focus on modified superradiance effects between two or four atoms with finite delay times. Using a numerically exact matrix-product-states approach, we explore both Markovian and non-Markovian regimes and highlight the significant influence of time-delayed feedback effects and the clear breakdown of assuming instantaneous coupling dynamics. We first show a system composed of two spatially separated qubits, prepared in a doubly excited state (both fully excited), and provide a comprehensive study of how delayed feedback influences the collective system decay rates, as well as the quantum correlations between waveguide photons, atoms, and between atoms and photons. The system is then extended to include two additional qubits located next to the initial ones (four qubits in total), and we demonstrate, by manipulating the initial excitations and the time-delay effects, how long-term quantum correlations and light-matter entangled states can be established.

DOI: [10.1103/szlz-d5dz](https://doi.org/10.1103/szlz-d5dz)

I. INTRODUCTION

Collective effects of radiatively coupled atoms and photon emitters [1] are important for understanding fundamental aspects of light-matter interactions beyond a single-dipole decay and have applications for producing entangled states, which is important for quantum technologies and quantum information processing. Manifestations of collective effects include the formation of Dicke states [2–4], Förster coupling, and fluorescence resonance energy transfer [5–7]. One of the most controlled environments for photon-coupled two-level systems (TLSs) is through waveguide modes, in an architecture known as waveguide quantum electrodynamics (QED) [8–23]. Waveguide QED systems offer spatial and temporal control over the interatom coupling rates and give rise to interesting quantum optical effects, such as enhanced spontaneous emission (SE) [24–26], including superradiance and directional emission control [27–30].

Many quantum optics models currently used to solve these many-body waveguide systems rely on the Markov approximation [31–35] and/or assume a weak-excitation regime [36,37], and thus often neglect important nonlinear interactions and atomic population effects [38–40], as well as photon-matter entanglement (Markov regime). There are several well-established approaches for accurately modeling few-photon transport in waveguide QED, including scattering solutions and input-output theories that go beyond the weak-excitation approximation (WEA) [36,41–50], but the dynamical observables can be difficult to extract directly, and often the Markov approximation is used to simplify calculations [51]. However, the neglect of time-retardation effects cannot capture time-delayed feedback effects [52], where more powerful techniques are needed, such as matrix product

states [53], space-discretized quantum trajectories [54], or analytical derivations of the differential equations for simpler systems [55].

While non-Markovian delay effects are often neglected for qubits in waveguides (instantaneous coupling), especially when not invoking a WEA, it has been shown that delayed feedback effects can greatly influence the TLS dynamics as one increases the distance between atoms [53,56–58]. This is especially noticeable when considering nonlinearities and dealing with fully quantized input fields [59,60]. Modeling such effects, i.e., including multiple quanta and finite time delays, is computationally challenging since, as the distance between the TLSs grows, so does the Hilbert space, and one has to treat the photons exactly, i.e., as part of the entire waveguide QED system.

The initial state in which correlated atoms are prepared will also directly affect their behavior, e.g., it is known that a pair of symmetrically entangled TLSs (superradiant state) [2, 61–64] will cause a faster SE decay of the atoms and it has been shown that finite distances between them can further enhance the atom SE decay, where a constructive relative phase between the atoms can lead to a collective emission higher than the usual superradiant one; this is the so-called superduperradiance [65]. Thus, finite delay effects can modify the usual understanding of Dicke states, where non-Markovian feedback effects are not taken into account, and N atoms starting in a symmetrical state have an initial temporal burst, enhancing their collective decay. In the Markovian case, a fully excited N -qubit system (i.e., starting with all atoms excited) will have a collective decay rate of [2,61]

$$W_N = N\gamma, \quad (1)$$

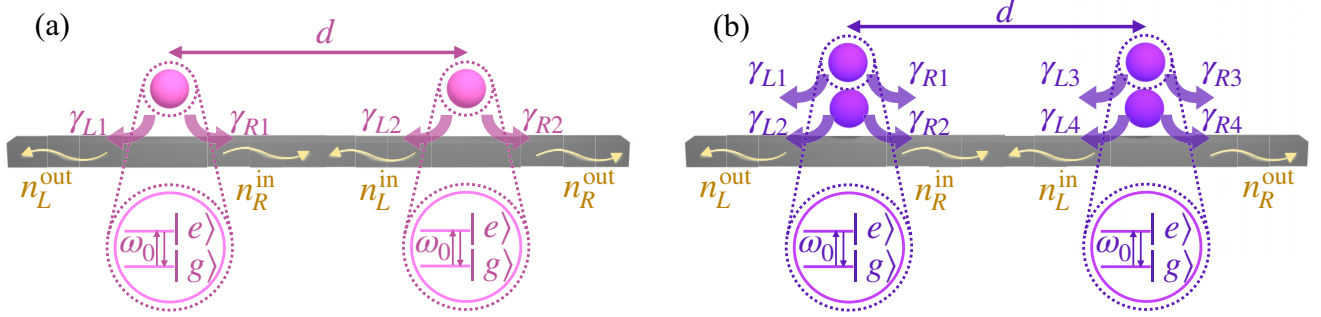


FIG. 1. (a) Schematic of two artificial atoms (treated as TLSs) in an infinite (open) waveguide, separated by a finite distance d . (b) Similar system to (a) but now with four TLSs, two in each of the groups.

while a half excited symmetrical initial state, where N is an even number, will have a decay rate of

$$W_{N/2} = \frac{N}{2} \left(\frac{N}{2} + 1 \right) \gamma, \quad (2)$$

and in the limit where there is only one initial excitation, the excitation will decay with

$$W_1 = N\gamma. \quad (3)$$

A. Finite delay effects in waveguide QED with two quantum excitations

In this work we investigate waveguide QED finite delay effects (yielding significant non-Markovian effects as experienced by the atoms) with a pair of TLSs prepared in an initial state with two quantum excitations (thus, beyond a simple linear response) and explore the role of finite delays as well as the effects of adding extra TLSs next to the initial pair. This is a first step for investigating the interactions between two clouds of TLSs separated by a finite distance. To solve this complex many-body problem, we use a tensor network approach [specifically, using matrix product states (MPS)] [53,66–71], which allows us to decompose a large Hilbert space into smaller subspaces and solve the problem in a numerically exact and efficient way. Therefore, we can fully include finite delay and feedback effects, nonlinearities, and a higher number of quantized excitations and easily extract useful information and observables for both the atoms and fields (quantized waveguide photons).

Although the collective response of identical atoms is a well-studied problem, it has been predominantly studied in the Markovian regime, thus ignoring finite delay feedback effects. These Markovian approaches fail when delay times become comparable to the lifetime of the TLSs (and often delay times with just a fraction of this lifetime can induce fundamentally new correlation effects [54]), which can have a pronounced effect on the quantum dynamics and quantum correlation functions. Fully non-Markovian dynamics have been studied mostly in the long-time limit [72,73] or considering a single excitation [65] (WEA). However, recent work [74] has exploited Laplace transform solutions to analytically solve the time dynamics of two atoms initially excited, separated by a distance $d = \tau v_g$, where τ is the delay time between them and v_g is the group velocity of the electromagnetic field; the authors show the probability of having one excitation versus

time, as well as the concurrence (atom-atom entanglement) and correlation between atomic dipoles. Although the feedback effects are clearly apparent in these three observables, the work also assumes that the probability of having two excitations is independent of the delay time. However, in our work we show how the two-atom excitation probability does depend on the finite feedback effects, and we significantly extend the study of such a system to explore other observables, thus gaining a deeper understanding of this problem. In addition, we also explore the role of adding in additional atoms, as discussed below.

B. Pair of two-level systems separated by a finite distance

In our study we first consider two TLSs separated by a finite distance d , shown in Fig. 1(a), where the two atoms start in a two-excitation superradiant state, with a destructive phase between both atoms; this case is intrinsically nonlinear. To highlight the physics of the finite delay effects, we solve the problem in two regimes, (i) in the Markovian limit (instantaneous coupling regime) and (ii) in the non-Markovian regime (with delayed feedback effects fully included), and investigate how the distance between the atoms affects the quantum dynamics.

We investigate not only the atom and field dynamics but also the correlations between them, calculating correlations between the two TLSs, field (photon) correlations and light-matter correlations that give us a deeper understanding of the dynamics, showing signatures of long-lasting light-matter entangled states. We also explore how finite delays affect the atomic excitations, modifying the doubly excited collective decay, contrary to previous findings in the literature, where the decay of a doubly excited state was independent of the distance between TLSs [74].

C. Multiatom waveguide QED results

In addition, we study multiatom waveguide QED results when the system is extended to include additional atoms located close to each of the initial TLS pair, as shown in Fig. 1(b), where we now have additional degrees of freedom when choosing an initial state. We will demonstrate significant deviations from the usual understanding of collective Dicke states in a Markovian regime, such as population trapping of the doubly excited state and photon trapping in the waveguide region between the TLS pair, thus offering a much richer

coupling regime with the non-Markovian coupling and control. We also show how adding one TLS next to each of the initial atoms affects the collective emission of the system. Here we can either add them as initial unexcited atoms and thus start the system in a product state or, alternatively, engineer new initial superradiant states, e.g., starting each pair in an entangled state with a shared excitation, which may enhance the collective SE decay rates, or maximize the field entanglement. Moreover, we calculate various other useful observables such as the transmitted or reflected photon fluxes and light-matter quantum correlations, including emitted spectra, to better understand the unique nature of these complex quantum systems.

The rest of our paper is organized as follows. In Sec. II we introduce our MPS theory, as well as the theoretical approach chosen to solve these waveguide QED problems, with the solution for two TLSs in a waveguide in Sec. II A and the extension to four TLSs (two pairs, spatially separated) in Sec. II B. Section III studies the time dynamical results for two TLSs, including a study of the delay dependence on the probability of atomic excitations in Sec. III A. In Sec. III B we further study the single atomic excitation as a function of the delay times as well as the atom-atom correlations. The role of the phase between atoms is investigated in Sec. III C. Additional quantum observables are calculated in Sec. III D, providing a comprehensive understanding of the system. In Sec. IV we analyze the influence of adding two new TLSs next to the previous ones, where we now have more degrees of freedom starting with an initially doubly excited state. Here we study again the collective decay rates and photon fluxes in the non-Markovian regime, showing long-lasting light-matter entangled states. We stress that all of our results are in the nonlinear two-excitation regime, in contrast to many previous works that restrict the solution to a one-photon subspace (which has a simple linear solution). In Sec. V we present a summary and general conclusions.

II. THEORETICAL DESCRIPTION

A. Pair of two-level systems in an infinite waveguide

A system consisting of two TLSs in an infinite waveguide [Fig. 1(a)] can be represented by the Hamiltonian [53] (units of $\hbar = 1$)

$$H = \sum_{n=1,2} H_{\text{TLS}}^{(n)} + H_W + H_I, \quad (4)$$

where the first term represents the TLSs

$$H_{\text{TLS}}^{(n=1,2)} = \omega_n \sigma_n^+ \sigma_n^-, \quad (5)$$

with ω_n the transition frequency and σ_n^+ and σ_n^- the relevant Pauli operators for TLS n . The waveguide term is

$$H_W = \sum_{\alpha=L,R} \int_{\mathcal{B}} d\omega \omega b_{\alpha}^{\dagger}(\omega) b_{\alpha}(\omega), \quad (6)$$

where $b_{\alpha}^{\dagger}(\omega)$ and $b_{\alpha}(\omega)$ are the creation and annihilation bosonic operators, respectively, for both right- and left-moving photons, and \mathcal{B} is the relevant bandwidth of interest around the resonance frequency ω_0 , in the rotating-wave approximation. Here we consider a waveguide initially in the vacuum state, i.e., with no initial photons. Finally, the last term

represents the interaction between the photons and qubits,

$$H_I = \frac{1}{\sqrt{2\pi}} \int_{\mathcal{B}} d\omega \left(\sum_{n=1,2} [\sqrt{\gamma_{L_n}} e^{i\omega x_n/c} b_L(\omega) \sigma_n^+ + \sqrt{\gamma_{R_n}} e^{-i\omega x_n/c} b_R(\omega) \sigma_n^+] + \text{H.c.} \right), \quad (7)$$

where x_1 and x_2 are the locations of each TLS in the waveguide, $d = x_2 - x_1$ is the distance between them, and $\tau = d/c$ is the delay time that it takes for a photon to travel from one TLS to the other (when separated by a distance d). Here we have assumed that the coupling frequency is close to the TLSs frequency and that the decay rates γ_L and γ_R to the left and right, respectively, do not depend on frequency. In addition, we assume no losses due to radiation leakage or qubit dephasing processes, which is a very good approximation when using semiconductor waveguides and circuit QED waveguides [75,76], at low temperatures, especially photonic crystal waveguides [26]. We also transform to the interaction picture with a rotating frame in terms of ω_0 . Next we transform the Hamiltonian to the interaction picture with respect to the free dynamics and then transform it to the time domain, where we change accordingly the boson operators [53], and use MPS to solve the problem, without performing any bath approximations.

Matrix product states is an approach based on tensor network methods that uses Schmidt decompositions or singular value decompositions to decompose the large Hilbert space of the entire system, including both the TLSs and the waveguide, into smaller subspaces. The significant advantage of this approach is that, once we have these smaller subspaces, we can apply the time-evolution operator only in the relevant parts of the system at each time step [68,77,78].

To proceed, we discretize the waveguide in time into the so-called time bins and write the discretized Hamiltonian in time [53,79,80]. Thus, we can write the time-evolution operator for each time step to evolve the whole system,

$$U(t_{k+1}, t_k) = \exp \left(-i \int_{t_k}^{t_{k+1}} dt' H(t') \right), \quad (8)$$

which in this case can be written as

$$\begin{aligned} U(t_{k+1}, t_k) &= \exp \left(-\{ [\sqrt{\gamma_{L_1}} \Delta B_L(t_k) + \sqrt{\gamma_{R_1}} \Delta B_R(t_{k-l}) e^{i\phi}] \sigma_1^+ + \text{H.c.} \} \right. \\ &\quad \left. - i\{ [\sqrt{\gamma_{L_2}} \Delta B_L(t_{k-l}) e^{i\phi} + \sqrt{\gamma_{R_2}} \Delta B_R(t_k)] \sigma_2^+ + \text{H.c.} \} \right) \end{aligned} \quad (9)$$

where $\Delta B_{R,L}^{\dagger} = \int_{t_k}^{t_{k+1}} dt' b_{R,L}^{\dagger}(t')$ and $\Delta B_{R,L} = \int_{t_k}^{t_{k+1}} dt' b_{R,L}(t')$ are the noise matrix product operators that create and annihilate, respectively, a photon in a time bin with a commutation relation

$$[\Delta B_{R,L}(t_k), \Delta B_{R,L}^{\dagger}(t_{k'})] = \Delta t \delta_{k,k'} \delta_{R,L}, \quad (10)$$

and $l = \tau/\Delta t$ represents the number of time bins between the two spatially-separated TLSs [53]. In the Markovian limit, $\tau = 0$, and everything is assumed to happen at the same time step (instantaneous coupling regime). The propagation phase ϕ between the two TLSs, in the interaction picture, is defined

as

$$\phi = -\omega_0 \tau. \quad (11)$$

Unless there is an external pump field, the number of excitations in the system should be conserved (at least within a rotating-wave approximation); hence, a conservation rule must be fulfilled. For example, considering two TLSs in the Markovian regime, the total number of excitations $N_{\text{total}}(t)$ for all time t is

$$\begin{aligned} N_{\text{total}}(t) &= n_{\text{TLS1}}(t) + n_{\text{TLS2}}(t) + \int_0^t [n_R^{\text{out}}(t') + n_L^{\text{out}}(t')] dt' \\ &= n_{\text{TLS1}}(t) + n_{\text{TLS2}}(t) + N_R^{\text{out}}(t) + N_L^{\text{out}}(t), \end{aligned} \quad (12)$$

where $n_{\text{TLS1}} = \langle \sigma_1^+ \sigma_1^- \rangle$ and $n_{\text{TLS2}} = \langle \sigma_2^+ \sigma_2^- \rangle$ are the emitter populations of the TLSs and $n_{R(L)}^{\text{out}}(t) = \langle b_{R(L)}^\dagger(t) b_{R(L)}(t) \rangle$ are the instantaneous photon fluxes, and $N_{R(L)}^{\text{out}}$ are the right (left) integrated. For example, if we start with both TLSs excited ($|\phi_0\rangle = |ee\rangle$), then $N_{\text{total}}(t) = 2$ at all times.

In the non-Markovian regime, the conservation rule will have two extra terms, since we now have to consider the possibility of having photons within the feedback loop, i.e., in the waveguide space between the qubits, and we now have

$$\begin{aligned} N_{\text{total}}(t) &= n_{\text{TLS1}}(t) + n_{\text{TLS2}}(t) + \int_0^t [n_R^{\text{out}}(t') + n_L^{\text{out}}(t')] dt' \\ &\quad + \int_{t-\tau}^t [n_R^{\text{in}}(t') + n_L^{\text{in}}(t')] dt' \\ &= n_{\text{TLS1}}(t) + n_{\text{TLS2}}(t) + N_R^{\text{out}}(t) \\ &\quad + N_L^{\text{out}}(t) + N_R^{\text{in}}(t) + N_L^{\text{in}}(t), \end{aligned} \quad (13)$$

where the new integral terms account for the photons within the feedback loop $N_{R,L}^{\text{in}}$. Once again, if we start with both fully excited TLSs, $N_{\text{total}}(t) = 2$ at all times.

Next we define the time evolution of the probability of having zero [$P^{(0)}(t)$], one [$P^{(1)}(t)$], or two [$P^{(2)}(t)$] atomic excitations in the waveguide system, where $P^{(0)}(t)$ corresponds to having both TLSs in the ground state, $P^{(1)}(t)$ is the probability of having one of them excited while the other one stays unpopulated, which in this case will be a combination of the probability of having either the left or right TLS populated, and $P^{(2)}(t)$ corresponds to having both TLSs populated:

$$P^{(0)}(t) = \langle \sigma_1^- \sigma_1^+ \sigma_2^- \sigma_2^+ \rangle(t), \quad (14)$$

$$P^{(1)}(t) = \langle \sigma_1^+ \sigma_1^- \sigma_2^- \sigma_2^+ \rangle(t) + \langle \sigma_1^- \sigma_1^+ \sigma_2^+ \sigma_2^- \rangle(t), \quad (15)$$

$$P^{(2)}(t) = \langle \sigma_1^+ \sigma_1^- \sigma_2^+ \sigma_2^- \rangle(t). \quad (16)$$

We can again write the conservation rule now in terms of these probabilities for the case with two excitations,

$$\begin{aligned} N_{\text{total}}(t) &= P^{(1)}(t) + 2P^{(2)}(t) + N_R^{\text{out}}(t) + N_L^{\text{out}}(t) \\ &\quad + N_R^{\text{in}}(t) + N_L^{\text{in}}(t) = 2, \end{aligned} \quad (17)$$

considering that in the Markovian limit $N_{R,L}^{\text{in}}(t) = 0$.

B. Two pairs of qubits (four TLSs) in an infinite waveguide

Next we consider two additional TLSs, next to the initial TLSs that we previously had; thus the system is now formed by two TLSs at each side [Fig. 1(b)], with four in total. The complete system Hamiltonian is now

$$H = \sum_{n=1,2,3,4} H_{\text{TLS}}^{(n)} + H_W + H_I, \quad (18)$$

with the interaction term

$$\begin{aligned} H_I &= \frac{1}{\sqrt{2\pi}} \int_B d\omega \left(\sum_{n=1,2} [\sqrt{\gamma_{L_n}} e^{i\omega x_L/c} b_L(\omega) \sigma_n^+ + \sqrt{\gamma_{R_n}} e^{-i\omega x_L/c} b_R(\omega) \sigma_n^+] + \text{H.c.} \right) \\ &\quad + \frac{1}{\sqrt{2\pi}} \int_B d\omega \left(\sum_{n=3,4} [\sqrt{\gamma_{L_n}} e^{i\omega x_R/c} b_L(\omega) \sigma_n^+ + \sqrt{\gamma_{R_n}} e^{-i\omega x_R/c} b_R(\omega) \sigma_n^+] + \text{H.c.} \right), \end{aligned} \quad (19)$$

where x_L and x_R represent the locations of the TLSs situated on the left and right, respectively, and $d = x_R - x_L$ is the distance between the pairs (as before).

The modified time-evolution operator is

$$\begin{aligned} U(t_{k+1}, t_k) &= \exp \left(-i \{ [\sqrt{\gamma_{L_1}} \Delta B_L(t_k) + \sqrt{\gamma_{R_1}} \Delta B_R(t_{k-1}) e^{i\phi}] \sigma_1^+ + \text{H.c.} \} \right. \\ &\quad - i \{ [\sqrt{\gamma_{L_2}} \Delta B_L(t_k) + \sqrt{\gamma_{R_2}} \Delta B_R(t_{k-1}) e^{i\phi}] \sigma_2^+ + \text{H.c.} \} \\ &\quad - i \{ [\sqrt{\gamma_{L_3}} \Delta B_L(t_{k-1}) e^{i\phi} + \sqrt{\gamma_{R_3}} \Delta B_R(t_k)] \sigma_3^+ + \text{H.c.} \} \\ &\quad \left. - i \{ [\sqrt{\gamma_{L_4}} \Delta B_L(t_{k-1}) e^{i\phi} + \sqrt{\gamma_{R_4}} \Delta B_R(t_k)] \sigma_4^+ + \text{H.c.} \} \right), \end{aligned} \quad (20)$$

and in the following sections we will consider identical atoms, with $\gamma_{Rn} = \gamma_{Ln} = \gamma/2$ (symmetric coupling), though this is not a model requirement.

If we study the system in terms of atomic excitations, in the case of still having two total excitations, the conservation rule still follows [Eq. (17)], but the atomic probabilities are now

$$P^{(0)}(t) = \langle \sigma_1^- \sigma_1^+ \sigma_2^- \sigma_2^+ \sigma_3^- \sigma_3^+ \sigma_4^- \sigma_4^+ \rangle(t), \quad (21)$$

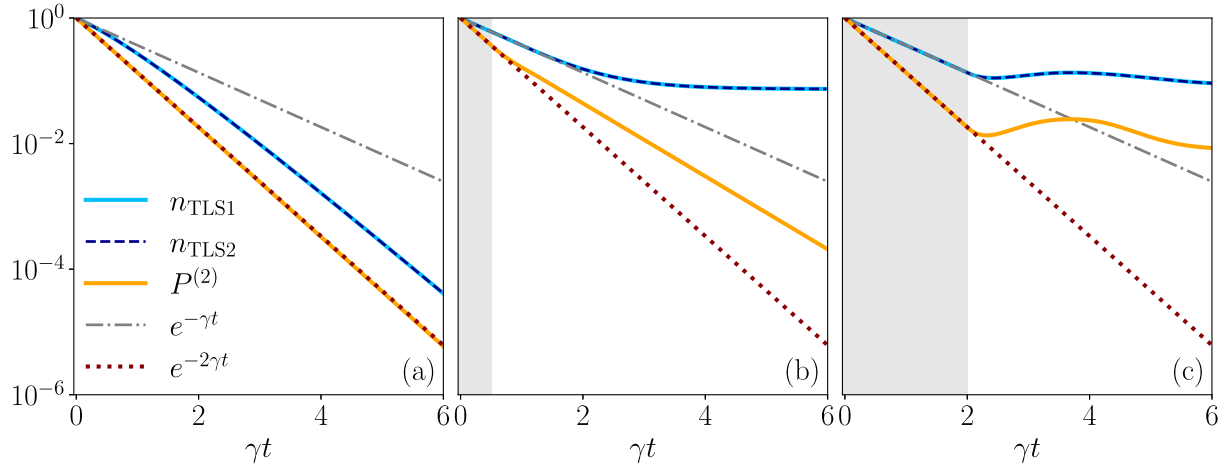


FIG. 2. Emitter population dynamics of two TLSs, initially excited, solved (a) in the Markovian regime and (b) then with a delay time of $\gamma\tau = 0.5$ and (c) with a delay time of $\gamma\tau = 2$. Individual TLS populations are shown in blue (solid and dashed lines), the probability of two atomic excitations $P^{(2)}(t)$ is in orange, and the analytical exponential decays for the Markovian regime are shown in (a), for reference, with the gray dash-dotted line and maroon dotted line for one and two initial excitations, respectively. The gray shaded area in (b) and (c) indicates the delay time τ when the non-Markovian dynamics begins to occur.

$$P^{(1)}(t) = \langle \sigma_1^+ \sigma_1^- \sigma_2^- \sigma_2^+ \sigma_3^- \sigma_3^+ \sigma_4^- \sigma_4^+ \rangle(t) + \langle \sigma_1^- \sigma_1^+ \sigma_2^+ \sigma_2^- \sigma_3^- \sigma_3^+ \sigma_4^- \sigma_4^+ \rangle(t) \\ + \langle \sigma_1^- \sigma_1^+ \sigma_2^- \sigma_2^+ \sigma_3^+ \sigma_3^- \sigma_4^- \sigma_4^+ \rangle(t) + \langle \sigma_1^- \sigma_1^+ \sigma_2^- \sigma_2^+ \sigma_3^- \sigma_3^+ \sigma_4^+ \sigma_4^- \rangle(t), \quad (22)$$

$$P^{(2)}(t) = \langle \sigma_1^+ \sigma_1^- \sigma_2^+ \sigma_2^- \sigma_3^- \sigma_3^+ \sigma_4^- \sigma_4^+ \rangle(t) + \langle \sigma_1^- \sigma_1^+ \sigma_2^+ \sigma_2^- \sigma_3^+ \sigma_3^- \sigma_4^- \sigma_4^+ \rangle(t) \\ + \langle \sigma_1^- \sigma_1^+ \sigma_2^- \sigma_2^+ \sigma_3^+ \sigma_3^- \sigma_4^+ \sigma_4^- \rangle(t) + \langle \sigma_1^+ \sigma_1^- \sigma_2^- \sigma_2^+ \sigma_3^- \sigma_3^+ \sigma_4^+ \sigma_4^- \rangle(t) \\ + \langle \sigma_1^+ \sigma_1^- \sigma_2^- \sigma_2^+ \sigma_3^+ \sigma_3^- \sigma_4^- \sigma_4^+ \rangle(t) + \langle \sigma_1^- \sigma_1^+ \sigma_2^+ \sigma_2^- \sigma_3^- \sigma_3^+ \sigma_4^+ \sigma_4^- \rangle(t). \quad (23)$$

With our MPS approach, we note that this can be easily extended to include the addition of more pairs of atoms located next to the current ones (or at other spatial locations as well).

In order to ensure numerical convergence in all of our results, we have limited the maximum bond dimension to d^2N , where d is the dimension of each time bin and is squared to account for the left- and right-moving photons. In all the cases studied here, we have two excitations in the system at all times; hence, the maximum bond dimension used is 8. The time step used in all the calculations is $\gamma\Delta t = 0.02$. Further details of our MPS approach and comparison with alternative techniques are discussed in detail in Ref. [53].

III. RESULTS FOR TWO COUPLED QUBITS WITH TWO EXCITATIONS

A. Finite delay dependence on the probability of atomic excitations with two qubits

We start by looking at two TLSs, initially excited, separated by a distance d [see Fig. 1(a)], and study the TLS population dynamics as well as how feedback effects can affect their decay rates.

In the Markovian regime, one has a traditional Dicke state and, as mentioned above, the collective decay rate simply depends on the number of TLSs and the initial number of initial excitations (with one excitation being inherently linear). Here we have two TLSs, hence $N = 2$, and particularly in

this case, if the system starts with one excitation, following Eq. (3), $W_1 = 2\gamma$; but if there are initially two excitations, from Eq. (1), $W_2 = 2\gamma$ too. This means that in the case of one excitation, the decay will be $P^{(1)}(t) = e^{-2\gamma t}$, and for two TLSs initially excited there is a collective decay $P^{(2)}(t) = e^{-2\gamma t}$.

Figure 2 shows the population dynamics of each atom decaying from an initially doubly excited state ($|\phi_0\rangle = |ee\rangle$) and the collective doubly excited atom decay [$P^{(2)}(t)$]. Figure 2(a) presents the Markovian dynamics matching the analytical decay of 2γ shown with the maroon dotted curve. We then consider delay-induced feedback effects, for two different delay times $\gamma\tau = 0.5$ and 2 in Figs. 2(b) and 2(c), respectively, with a phase $\phi = 0$ in both cases. With a time-delayed feedback, we observe the trapping of the TLS populations, and with the longer delay time, we can also observe oscillations due to the partial reexcitation of the TLSs; this oscillation time corresponds to the photon round-trip time, which is clearly a significant delay-induced dynamic.

We also observe how the probability of having two atomic excitations is highly affected by the feedback effects, even with the shorter delay time. This is in contrast to previous work reported in Ref. [74], which derives $P^{(2)}(t) = e^{-2\gamma t}$, and states that the probability of having two atomic excitations is independent of the delay between atoms. However, Fig. 2 clearly shows that it does depend on the delay times, and it becomes significant for larger delay times. It is important to also note that we have calculated the conservation rule, using

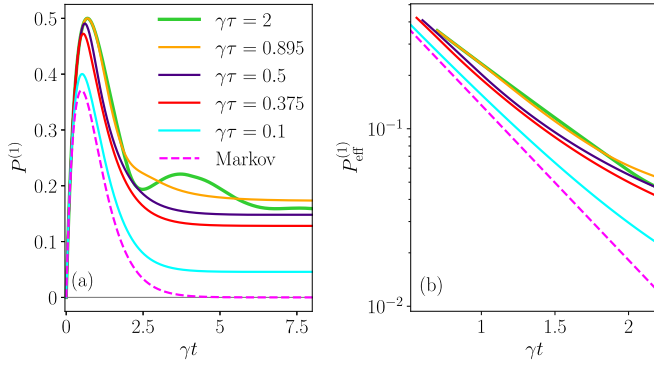


FIG. 3. Time dynamics of two atoms initially excited. (a) Probability of having only one of the TLSs excited, i.e., probability of one atomic excitation $P^{(1)}(t)$, for different delay times, when the system is initialized with both TLSs excited. (b) Close-up of the reduced probability of having only one of the TLSs excited $P_{\text{eff}}^{(1)}(t)$ on a logarithmic scale, for the different delay times plotted in (a).

both the individual TLS populations [see Eq. (13)] and the collective atomic excitations [see Eq. (17)], in order to confirm the validity of our results.

B. Further analysis of the one atomic excitation probability $P^{(1)}$ and atom-atom correlations

To more fully explore the non-Markovian effects of our system, we also search for interesting delay times (or atom separations) that can lead to interesting temporal effects that qualitatively change because of finite delay coupling regimes between the emitters. In Ref. [74], for the case of two atoms initially excited, the authors studied two specific lengths that were cited to correspond to the largest instantaneous decay rate ($\gamma\tau = 0.375$) and the maximum probability of having one atomic excitation in the long-time limit, $\max P^{(1)}(t \rightarrow \infty)$ ($\gamma\tau = 0.895$).

To have a more complete picture, we study $P^{(1)}(t)$ for a number of different delay times in Fig. 3(a), including the ones mentioned above. We observe that, as stated in Ref. [74], $\gamma\tau = 0.895$ indeed gives the highest value of $P^{(1)}(t)$ at long times. However, it is not clear that the delay time of $\gamma\tau = 0.375$ yields the largest instantaneous decay rate, since in Fig. 3(a) this does not appear to be the case.

In the Markovian regime, $P^{(1)}(t)$ has a known analytical solution $P^{(1)}(t) = 2\gamma t e^{-2\gamma t}$ [61]. Thus, we can define $P_{\text{eff}}^{(1)}(t) = P^{(1)}(t)/2\gamma t$ to extract its effective decay rate, which in this case will be 2γ . Of course, this assumes the solution remains Markovian, so the results below are only for a qualitative understanding of the effective decay rates. In Fig. 3(b) we show $P_{\text{eff}}^{(1)}(t)$ for the same results shown in Fig. 3(a), on a logarithmic scale. First, we see how, as expected, the Markovian result is a straight line with a slope of 2γ . Second, we observe how feedback effects create new nonlinearities and the decay rates are time dependent; however, we do not see an especially faster decay for $\gamma\tau = 0.375$.

To help study the underlying physics of these different delays and how they affect the interemitter coupling, in Fig. 4 we calculate the emitter-emitter correlation function, specifically $\langle\sigma_1^+\sigma_2^-\rangle(t)$, in order to compare with and extend previous atom-atom correlation results from Ref. [74]. We highlight that our findings appear to differ from the ones reported in [74]. Figure 4 shows the atomic correlations for two different delay times $\gamma\tau = 0.375$ [Fig. 4(a)] and $\gamma\tau = 0.895$ [Fig. 4(b)]. First, when we look at the $\gamma\tau = 0.895$ case with $\phi = (2n+1)\pi$ solution, which corresponds to the blue solid curve in Fig. 4(b); we observe different time dynamics, with only positive values of the atomic correlations. However, if we now calculate this atomic correlation function for $\gamma\tau = 0.375$ [blue solid line in Fig. 4(a)], the time dynamics follow a similar shape to the case reported in Ref. [74], Fig. 3(b) therein, but with their simulated delay time of $\gamma\tau = 0.895$. In our Fig. 4, when considering $\gamma\tau = 0.375$ with, say, $\phi = \pi$

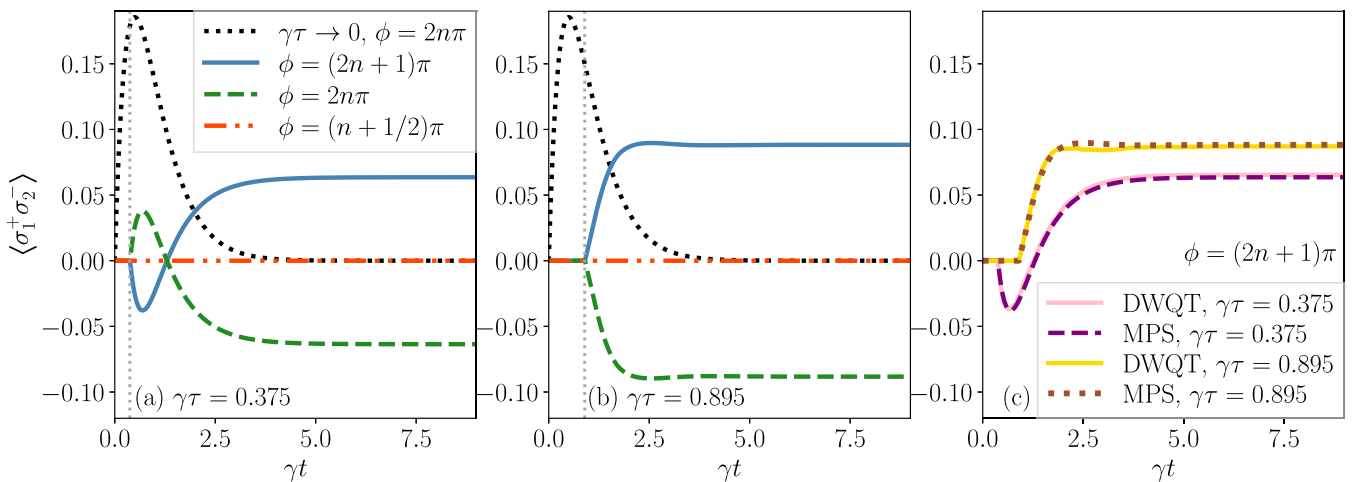


FIG. 4. Interemitter quantum correlations calculated using MPS for two TLSs separated by (a) $\gamma\tau = 0.375$ and (b) $\gamma\tau = 0.895$, where we distinguish between even and odd multiples of π for the phase, $\phi = 2n\pi$ and $\phi = (2n+1)\pi$. The Markov limit $\gamma\tau \rightarrow 0$ is shown for comparison. Since some of these results differ qualitatively from those in [74] (see the text for details), we have also computed some of these observables with a completely different method, specifically a discretized waveguide quantum trajectory approach [53,54], and results are shown in (c) for $\phi = (2n+1)\pi$, along with MPS results; the DWQT approach uses 20 000 quantum trajectories for averaging and clearly yields the same answer (with some minor noise due to trajectory averaging).

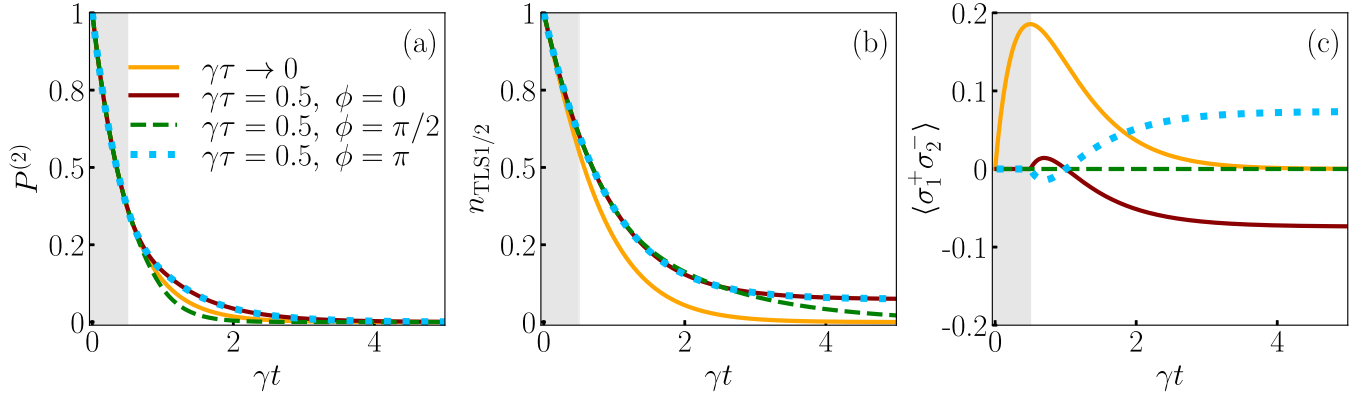


FIG. 5. Role of propagation phase on (a) collective decay $P^{(2)}$, (b) individual populations $n_{\text{TLS}1/2}$, and (c) atom-atom correlation $\langle \sigma_1^+ \sigma_2^- \rangle$ for a delay time of $\gamma\tau = 0.5$ and three different phases $\phi = 0$ (brown solid line), $\phi = \pi/2$ (green dashed line), and $\phi = \pi$ (blue dotted line). The Markovian solution is plotted in orange for comparison.

(blue solid line), the atomic correlation goes to negative values immediately after the finite delay time and then transitions to positive values at longer times, similar to the solution presented in Fig. 3(b) of [74], again with their longer delay time of $\gamma\tau = 0.895$, except for an earlier start (i.e., when we first see a temporal change) in our results due to the shorter delay time.

To further confirm that our simulations are correct, our results have been benchmarked with an independent approach using a discretized waveguide quantum trajectory (DWQT) model [53,54]. Agreement between both methods, MPS and DWQT, is shown in Fig. 4(c) for the two delay times studied in Figs. 4(a) and 4(b). Minor differences are caused by trajectory averaging in the DWQT method, where we use 20 000 trajectories.

Furthermore, we note that one has to be careful when choosing a value of m for the $\phi = m\pi$ phase. Here we find that there is a difference in the results between an even or odd value of m , with a flip on the sign when m is even. This is shown in Fig. 4 with green dashed curves. Additionally, for phases $\phi = \frac{(2m+1)\pi}{2}$ (red dash-dotted curves), there is no emitter-emitter correlation and $\langle \sigma_1^+ \sigma_2^- \rangle(t) = 0$ at all times.

C. Phase dependence in the non-Markovian regime

In the regime of time-delayed feedback, the phase term ϕ , defined earlier in Eq. (11), plays an important role in the time dynamics of the system, since it can control the onset of enhanced or suppressed atom decays. To appreciate the role of ϕ , we have also investigated the impact on $P^{(2)}$, $n_{\text{TLS}1/2}$, and $\langle \sigma_1^+ \sigma_2^- \rangle$ for a delay time of $\gamma\tau = 0.5$ and compared with the Markovian result.

First, in Fig. 5(a) we show collective decay $P^{(2)}$ for three phases, $\phi = 0$ (brown solid curve), $\phi = \pi/2$ (green dashed curve), and $\phi = \pi$ (blue dotted curve), and compare it with the results in the Markovian regime. As we already saw in Sec. III A, $P^{(2)}$ depends on τ in the non-Markovian regime and thus it will also depend on ϕ . Interestingly, we observe how the collective decay is enhanced for a phase of $\phi = (m +$

$1/2)\pi$, contrary to solutions with a single excitation, where the superradiant state is enhanced for a phase $\phi = 2m\pi$ [65].

Figure 5(b) shows the individual populations $n_{\text{TLS}1/2}$, where the dynamics remain the same for both atoms, since they start in a symmetrical state and have symmetrical decay rates. For this observable, the fastest decay is observed in the Markovian solution, and $\phi = \pi/2$ does not decay faster than the other phases. The main difference that can be observed here is the population trapping for the phases $\phi = \pi$ and $\phi = 0$, which is not present in the case of $\phi = \pi/2$.

Finally, in Fig. 5(c) we show the time-dependent atom-atom correlations $\langle \sigma_1^+ \sigma_2^- \rangle$ for the same phases. In this case, we see how atomic correlations are present even in the Markovian regime, except for $\phi = \pi/2$, which shows a perfect cancellation of the correlations between atoms. This again shows the dependence on the phase for the system evolutions, in agreement with the results in Ref. [74].

D. Additional quantum observables and non-Markovian effects

To better appreciate the role of non-Markovian effects on photons, we next extend our study to include observables related to the explicit behavior of waveguide photons and study both light-light and light-matter correlations.

In Fig. 6 we show a detailed summary of populations, correlations, and entanglement entropies (introduced and defined below), first starting in the Markovian regime [Figs. 6(a)–6(c)] and then with three different finite delay times $\gamma\tau = 0.1$ [Figs. 6(d)–6(f)], $\gamma\tau = 0.5$ [Figs. 6(g)–6(i)], and $\gamma\tau = 2$ [Figs. 6(j)–6(l)]. In the left column, the population dynamics are shown for both individual TLSs and collective atomic excitations $P^{(n)}$. Here we observe, as before, the pronounced time-delayed feedback effects in the non-Markovian cases, where the atoms decay individually until the delay time and then trapping of the TLS populations appears for longer times. Once again, with non-Markovian feedback, qualitatively different dynamics are observed for all $P^{(0)}$, $P^{(1)}$, and $P^{(2)}$. This is especially noticeable in the last two longer-delay cases [Figs. 6(g) and 6(j)], where we have longer delay times $\gamma\tau = 0.5$ and 2, respectively.

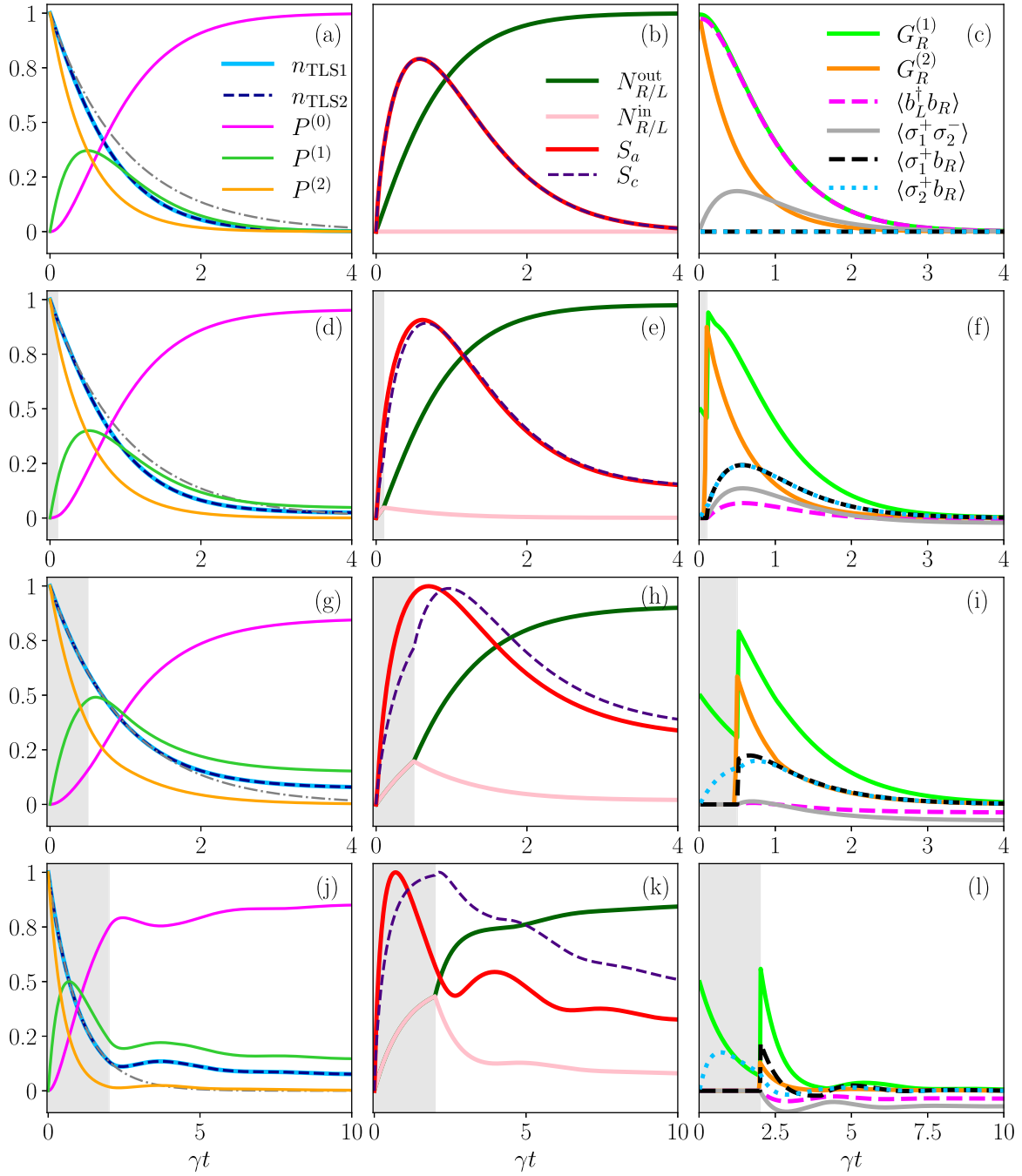


FIG. 6. Plot summarizing various important observables for four different cases, (a)–(c) the Markovian regime, (d)–(f) $\gamma\tau = 0.1$, (g)–(i) $\gamma\tau = 0.5$, and (j)–(l) $\gamma\tau = 2$, showing (a), (d), (g), and (j) the atomic population dynamics (single TLS decay represented with the gray dash-dotted curve for reference); (b), (e), (h), and (k) photon fluxes and entanglement entropies; and (c), (f), (i), and (l) correlations between operators in the system.

The middle column figures show the integrated output flux of photons going to the left and right of the waveguide, $N_{R,L}^{\text{out}}$ (dark green line), and the photon flux within the feedback loop, $N_{R,L}^{\text{in}}$ (pale pink line), defined in Eqs. (12) and (13). In this case, there is symmetry in the system; hence, the right- and left-moving photons will behave similarly. Here we can see how, as the distance between the atoms increases (longer delay times), the output photon flux gets smaller at

longer times. This is not only due to the trapped populations in the atoms, but also due to emerging probabilities of photons trapped in the feedback loop represented by $N_{R,L}^{\text{in}}$. We stress that this observation is unique to the non-Markovian regime, since in the Markovian limit, the feedback loop is not considered.

In Figs. 6(b), 6(e), 6(h), and 6(k) we also show the entanglement entropy, which is calculated in two different ways.

First, we define the entanglement entropy between the atomic and the photonic part of the system, from [56]

$$S_a = - \sum_{\beta} \Lambda(\text{sys})_{\beta}^2 \log_2 [\Lambda(\text{sys})_{\beta}^2], \quad (24)$$

where $\Lambda(\text{sys})_{\beta}$ are the Schmidt coefficients corresponding to the TLSs system bin, with β representing the position of these coefficients, and the subscript a on S_a stands for atomic. To ensure a maximum value of 1, this is normalized as $S_a = S_a/S_{\max}$, where $S_{\max} = n_{\text{qubits}} \log_2 2$. Second, we define the entanglement entropy of the entire circuit S_c , which corresponds to the entropy between the circuit considered (the two TLSs plus the feedback or waveguide between them) and the rest of the waveguide,

$$S_c = - \sum_{\beta} \Lambda(\tau)_{\beta}^2 \log_2 [\Lambda(\tau)_{\beta}^2], \quad (25)$$

where now $\Lambda(\tau)_{\beta}$ are the Schmidt coefficients of the feedback bin, and follow the same normalization $S_c = S_c/S_{\max}$.

In the Markovian regime, both (entanglement) entropies introduced above behave in the same manner because there is no feedback loop, as shown in Fig. 6(b), and they simply increase to a certain value and return to zero at sufficiently long times. However, as the feedback delay times increase [see Figs. 6(e), 6(h), and 6(k)] so does the difference between these two observables, reflecting the increase in the probability of having photons trapped between the two TLSs. Moreover, the entropy values are no longer zero at long times, showing long-term light-matter entanglement. We can also observe oscillations in the entropy for long delay times ($\gamma\tau = 2$), becoming clearer for S_a .

Figures 6(c), 6(f), 6(i), and 6(l) show different types of quantum correlations. We first have the photonic correlations, which are represented by the (one-time) first- and second-order quantum correlation functions $G_R^{(1)}(t)$ and $G_R^{(2)}(t)$ of the right output photons and the correlation between right- and left-moving photons $\langle b_L^{\dagger} b_R \rangle(t)$. In the Markov limit, the first-order correlation function and $\langle b_L^{\dagger} b_R \rangle(t)$ are the same due to the symmetry of the system, but this is no longer the case when there are finite delay feedback effects, where now the system behaves like two separated single-excited TLSs until the delay time τ , giving rise to different dynamics. This initial independent behavior is also reflected in the behavior of $G_R^{(2)}(t)$, which remains zero until $t = \tau$.

The two-atom correlation is also plotted in Figs. 6(c), 6(f), 6(i), and 6(l). Once again, here we can see the difference between the Markovian regime, where there is an instantaneous correlation between the TLSs, and the non-Markovian one, where the correlation between atoms does not start until the delay time and shows different dynamics depending on the atom distance, with negative correlation values for TLSs that are further apart.

Finally, we highlight that there are two more important observables shown in these figures, corresponding to the light-matter correlations between the first TLS and the right-moving photons, $\langle \sigma_1^+ b_R \rangle$, and the second TLS and the right-moving photons, $\langle \sigma_2^+ b_R \rangle$. These two observables remain zero in the Markovian regime, where the light-matter entanglement is not present, and become different from zero when

the feedback effects come into place, even when considering relatively short delay times like $\gamma\tau = 0.1$. This reinforces the fact that non-Markovian effects give rise to important light-matter entanglement not captured when considering certain approximations, and these can be measured from various correlation functions.

IV. FOUR COUPLED QUBITS WITH TWO EXCITATIONS

Next we can extend our two-atom study by adding a new pair of two TLSs, i.e., four TLSs in total, and investigate how the dynamics differ from the previous cases. For this system, we study a delay time of $\gamma\tau = 0.5$, where the delay effects are clearly visible but do not carry the oscillations of more extreme delay cases.

In terms of the initial state, even if considering the same number of initial excitations (two atomic excitations), there are now several options for the initial quantum state of the system since the two new TLSs add more degrees of freedom. Here we choose three example initial quantum states that we believe are especially interesting and relevant, but we remark that we can easily initialize the TLSs with any product state or entangled state containing two excitations or, in a more general case, containing up to four excitations.

Initial state A (one specific left atom excited and one specific right atom excited). Previously, for the case of two TLSs separated by a delay time τ , initially excited, we had an initial atomic state $|e_L, e_R\rangle$, where e_L represented the excited TLS on the left and e_R the excited one on the right. Now we can add two additional TLSs, both starting in the ground state, and see how these affect the collective dynamics of the system. In this case, we have the initial state

$$|\phi_0\rangle_A = |e_{1L}, g_{2L}, e_{1R}, g_{2R}\rangle. \quad (26)$$

Initial state B (two left atoms excited). In the Markovian regime, when considering that the phase between TLSs is $\phi = 0$, there is no difference for an initial product state with two excitations when choosing which two TLSs are excited. However, this is no longer the case when considering delay times. It is thus interesting to study the differences with an initial state where the two atomic excitations are on the left TLSs, since this case is only equivalent to the previous one (state A) in the Markovian limit. Here we will have an initial state

$$|\phi_0\rangle_B = |e_{1L}, e_{2L}, g_{1R}, g_{2R}\rangle. \quad (27)$$

Initial state C (one unknown left atom excited and one unknown right atom excited). In the previous examples, we assume that we know what precise TLSs are excited, but what happens if we only know that there is one excitation on the left and one on the right? The initial state will be a combination of all the possible initial states with two excitations,

$$|\phi_0\rangle_C = \frac{1}{2}(|e_{1L}, g_{2L}, e_{1R}, g_{2R}\rangle + |g_{1L}, e_{2L}, e_{1R}, g_{2R}\rangle + |g_{1L}, e_{2L}, g_{1R}, e_{2R}\rangle + |e_{1L}, g_{2L}, g_{1R}, e_{2R}\rangle). \quad (28)$$

This case is particularly interesting since, if we rearrange the terms, we can also write the initial state as

$$|\phi_0\rangle_C = \frac{1}{2}(|e_{1L}, g_{2L}\rangle + |g_{1L}, e_{2L}\rangle) \otimes (|e_{1R}, g_{2R}\rangle + |g_{1R}, e_{2R}\rangle), \quad (29)$$

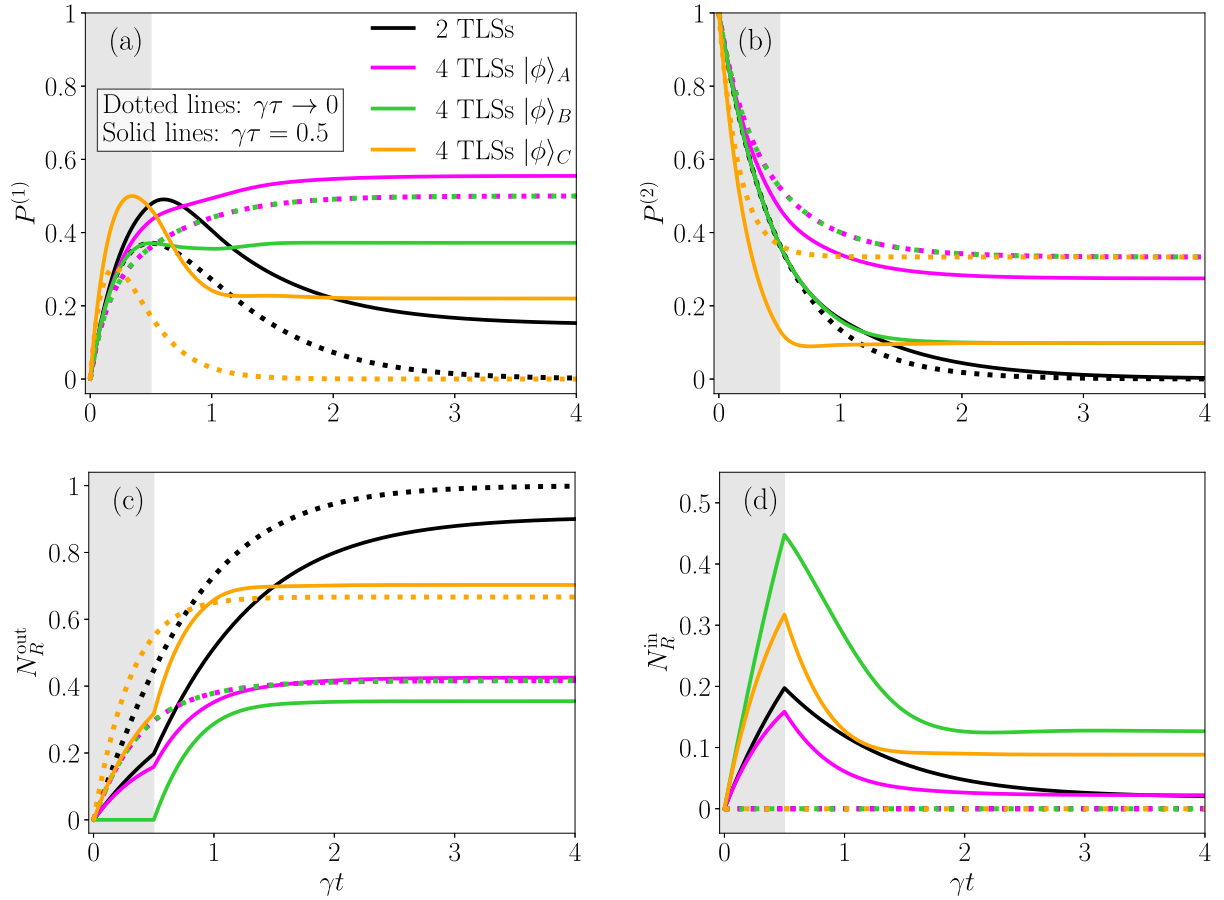


FIG. 7. (a) Probability of having one atomic excitation. (b) Probability of having two atomic excitations. (c) Integrated photon flux transmitted to the right. (d) Photon probability between the left and right TLS pairs. Magenta lines correspond to state A ($|\phi\rangle_A$), green lines to state B ($|\phi\rangle_B$), orange lines to state C ($|\phi\rangle_C$), and black lines to the two-excitation two-TLS solution previously studied. In all cases, the solid lines correspond to a delay time of $\gamma\tau = 0.5$ and the dotted lines are in the Markovian limit.

which corresponds to a product of a one-excitation superradiant state of the left TLSs and a one-excitation superradiant state with the TLSs on the right, and we can observe superradiant features in the collective population dynamics.

The time-dependent quantum dynamics of these three cases are summarized in Fig. 7, where state A ($|\phi\rangle_A$) is shown in magenta, state B ($|\phi\rangle_B$) in shown in green, and state C ($|\phi\rangle_C$) is shown in orange. For comparison, the results for two TLSs with two excitations are shown in black. Solid curves display non-Markovian results and dashed lines display Markovian results.

Several interesting features are observed. First, in Fig. 7(a) we can see how $|\phi\rangle_C$ behaves closer to the two-TLS case separated by a distance d [see Fig. 1(a)], in both the Markovian and non-Markovian cases, where in the Markovian limit the probability of one atomic excitation is zero in the long-time limit, but it reaches a constant in the non-Markovian regime. For the initial state $|\phi\rangle_C$, the dynamics are faster with four TLSs, since this is a double superradiant state and, for the same delay time, it reaches a higher constant value. However, $|\phi\rangle_A$ and $|\phi\rangle_B$ have totally different dynamics from the two-TLS solution, both with and without considering the delay times. As expected, in the Markovian limit, the dynamics of

$|\phi\rangle_A$ and $|\phi\rangle_B$ are the same, but when feedback effects come into place they deviate, with an increasing $P^{(1)}(t)$ for $|\phi\rangle_A$ and decreasing values for $|\phi\rangle_B$.

In Fig. 7(b) we first see how with two TLSs, the probability of two atomic excitations is zero for long times (in both regimes), since photons escape into the external waveguide parts. However, when adding the extra two TLSs (four in total), the two-excitation probability gets trapped in both the Markovian and non-Markovian regimes, as some waveguide photons are now trapped. This trapping in the Markovian regime is due to the fact that with four TLSs, even if we consider that their distance is small enough that we can disregard the feedback effects, we are still distinguishing the left and right pair of qubits. A fully superradiant state in which the two excitations were unknown within the four TLSs would not have long-lasting atomic excitations in the Markovian regime. In these cases, even though there are superradiant features, especially in state C, the distinction between pairs gives rise to atomic excitation trapping, even in the Markov limit.

Interestingly, in all the Markovian cases, the constant value for two atomic excitations at longer times is exactly the same value $P^{(2)} \approx 0.33$, although it initially decays much faster if the initial state is $|\phi\rangle_C$, since again this is

a combination of superradiant states. However, when considering the time-delayed feedback, we have three different collective decay rates. First, for $|\phi\rangle_A$, we have two separated pairs of TLSs with one excitation on each side before the delay time, which has the slowest rate, although this rate is still faster than the Markovian regime equivalent, and after the delay time both rates seem to become equal. Second, $|\phi\rangle_B$ has the same dynamics as the two-TLS case studied before ($\gamma\tau = 0.5$), with a decay rate of 2γ , since both excitations are on the left atoms, and after this time, the probability of having the two atomic excitations reaches a constant, smaller than in the previous case. Finally, $|\phi\rangle_C$ has a decay rate of 4γ , having the fastest dynamics, and it reaches a trapped state after the delay time τ , similar to the previous one.

Figures 7(c) and 7(d) show the photon dynamics of the system, with Fig. 7(c) showing the right output photon flux N_R^{out} and Fig. 7(d) the photon probability in the waveguide part between the TLS pairs for the right-moving photons N_R^{in} , defined previously. From the simulations with four TLSs, $|\phi\rangle_A$ has a low transmitted photon flux and the lowest probability of having photons trapped between the TLS pairs, which agrees with the fact that both the one- and two-atomic-excitation probabilities are higher than in the rest of cases. In contrast, $|\phi\rangle_B$ has fewer transmitted photons (with zero transmission until the photons reach the right pair of atoms when considering feedback), but it has the highest probability of having photons trapped between TLSs in the non-Markovian regime. The last case studied corresponding to $|\phi\rangle_C$ shows the largest transmission, with an even higher value when considering feedback effects, which, together with a high $P^{(1)}(t \rightarrow \infty)$ and the lowest $P^{(2)}(t \rightarrow \infty)$, makes it a good example of a long-term light-matter entangled state.

V. CONCLUSION

Using a powerful MPS approach, we have studied the effects of having finite delay times in the quantum dynamics of waveguide QED systems with multiple two-level atoms, with finite spatial separations, when they are prepared in superradiant states containing two atomic excitations. This is an intrinsically nonlinear problem, and we have shown how the collective decay rates are significantly modified with larger distances between atoms and studied the impact on various light-matter correlations and the entanglement between the TLSs and the field propagating in the waveguide. We have also demonstrated the clear breakdown of assuming instantaneous coupling rates, leading to much richer collective effects than for a Markovian system.

Starting with two TLSs, we first studied the influence of finite delay feedback effects on the double-excited state dynamics (superradiance regime) and on the emitter-emitter correlations. We showed how the superradiant coupling is delayed by the causality propagation time, manifesting in several non-Markovian decay regimes and long-lived emitter-photon decay rates. Our theory fully includes the waveguide photon dynamics including the effects of round-trip photons and population trapped states.

We then extended our study to present a more detailed analysis of the quantum dynamics by calculating other ob-

servables, including entanglement entropy and light-matter correlations, and several of these correlations are unique only in the non-Markovian regime, which is accessible in quantum circuits. For example, photon-matter correlation effects are zero for the Markovian coupling regime (which assumes zero feedback time), but significant in the presence of finite delays. In addition, the entanglement entropy between the atomic and photonic part (S_a) and the entanglement entropy between the circuit considered and the rest of the waveguide (S_c) are equivalent in the Markovian regime, since the photonic region between TLSs is not considered, but we have shown how they qualitatively differ as delay times increase and the probability of photons in that region becomes larger.

Finally, to explore additional new waveguide QED superradiant regimes with more qubits, we then added two more atoms to the waveguide, next to the original pair (thus having four qubits in total), and we again investigated their time dynamics when finite delay feedback effects occur. Here we have shown that, depending on the choice of our initial state, we can achieve different quantum dynamics, including long-lived light-matter entanglement. Here we found trapping of the collective doubly excited state with finite values at long times, in contrast to the two-TLS dynamics. We also observed trapping of the photons located between the TLSs. We have shown how these characteristics can be engineered with different initial states, making this a very rich system for creating light-matter entangled states.

We stress that our general theory can easily include additional photons and qubits, allowing us to explore waveguide-mediated quantum coherence and entanglement generation in multiatom waveguide QED systems, including cascaded chiral systems [81].

ACKNOWLEDGMENTS

This work was supported by the Natural Sciences and Engineering Research Council of Canada, the National Research Council of Canada, the Canadian Foundation for Innovation, and Queen's University, Canada. S.H. and S.A.R. acknowledge RIKEN for support, and S.H. thanks the Japanese Society for the Promotion of Science for an Invitational Fellowship. F.N. was supported in part by the Japan Science and Technology Agency (via the CREST Quantum Frontiers program Grant No. JPMJCR24I2, the Quantum Leap Flagship Program, and the Moonshot R&D Grant No. JPMJMS2061) and the U.S. Office of Naval Research Global (via Grant No. N62909-23-1-2074). We thank Gavin Crowder for supplying an independent check of some of the results shown in Fig. 4, using quantum trajectory theory. We thank Alberto Del Ángel Medina and Anton Frisk Kockum for valuable comments and insightful discussions. We also appreciate comments from Pablo Solano, Kanu Sinha, and Pablo Barberis-Blostein.

DATA AVAILABILITY

The data that support the findings of this article are not publicly available upon publication because it is not techni-

cally feasible and/or the cost of preparing, depositing, and hosting the data would be prohibitive within the terms of this

research project. The data are available from the authors upon reasonable request.

- [1] Z. Ficek and R. Tanaś, Entangled states and collective non-classical effects in two-atom systems, *Phys. Rep.* **372**, 369 (2002).
- [2] R. H. Dicke, Coherence in spontaneous radiation processes, *Phys. Rev.* **93**, 99 (1954).
- [3] S. Das, G. S. Agarwal, and M. O. Scully, Quantum interferences in cooperative Dicke emission from spatial variation of the laser phase, *Phys. Rev. Lett.* **101**, 153601 (2008).
- [4] N. Shammah, S. Ahmed, N. Lambert, S. De Liberato, and F. Nori, Open quantum systems with local and collective incoherent processes: Efficient numerical simulations using permutational invariance, *Phys. Rev. A* **98**, 063815 (2018).
- [5] Th. Förster, Zwischenmolekulare energiewanderung und fluoreszenz, *Ann. Phys. (Leipzig)* **437**, 55 (1948).
- [6] S. Ravets, H. Labuhn, D. Barredo, L. Béguin, T. Lahaye, and A. Browaeys, Coherent dipole–dipole coupling between two single Rydberg atoms at an electrically-tuned Förster resonance, *Nat. Phys.* **10**, 914 (2014).
- [7] D. L. Andrews, C. Curutchet, and G. D. Scholes, Resonance energy transfer: Beyond the limits, *Laser Photonics Rev.* **5**, 114 (2011).
- [8] J.-T. Shen and S. Fan, Strongly correlated multiparticle transport in one dimension through a quantum impurity, *Phys. Rev. A* **76**, 062709 (2007).
- [9] J.-T. Shen and S. Fan, Strongly correlated two-photon transport in a one-dimensional waveguide coupled to a two-level system, *Phys. Rev. Lett.* **98**, 153003 (2007).
- [10] D. Witthaut and A. S. Sørensen, Photon scattering by a three-level emitter in a one-dimensional waveguide, *New J. Phys.* **12**, 043052 (2010).
- [11] D. Roy, Two-photon scattering by a driven three-level emitter in a one-dimensional waveguide and electromagnetically induced transparency, *Phys. Rev. Lett.* **106**, 053601 (2011).
- [12] E. Sanchez-Burillo, D. Zueco, J. J. Garcia-Ripoll, and L. Martin-Moreno, Scattering in the ultrastrong regime: Nonlinear optics with one photon, *Phys. Rev. Lett.* **113**, 263604 (2014).
- [13] G. Calajó, F. Ciccarello, D. Chang, and P. Rabl, Atom-field dressed states in slow-light waveguide QED, *Phys. Rev. A* **93**, 033833 (2016).
- [14] S. Hughes, Enhanced single-photon emission from quantum dots in photonic crystal waveguides and nanocavities, *Opt. Lett.* **29**, 2659 (2004).
- [15] H. Zheng, D. J. Gauthier, and H. U. Baranger, Waveguide QED: Many-body bound-state effects in coherent and Fock-state scattering from a two-level system, *Phys. Rev. A* **82**, 063816 (2010).
- [16] A. F. Kockum, G. Johansson, and F. Nori, Decoherence-free interaction between giant atoms in waveguide quantum electrodynamics, *Phys. Rev. Lett.* **120**, 140404 (2018).
- [17] B. Kannan, M. J. Ruckriegel, D. L. Campbell, A. Frisk Kockum, J. Braumüller, D. K. Kim, M. Kjaergaard, P. Krantz, A. Melville, B. M. Niedzielski, A. Vepsäläinen, R. Winik, J. L. Yoder, F. Nori, T. P. Orlando, S. Gustavsson, and W. D. Oliver, Waveguide quantum electrodynamics with superconducting artificial giant atoms, *Nature (London)* **583**, 775 (2020).
- [18] J. R. Johansson, G. Johansson, C. M. Wilson, and F. Nori, Dynamical casimir effect in a superconducting coplanar waveguide, *Phys. Rev. Lett.* **103**, 147003 (2009).
- [19] J. R. Johansson, G. Johansson, C. M. Wilson, and F. Nori, Dynamical casimir effect in superconducting microwave circuits, *Phys. Rev. A* **82**, 052509 (2010).
- [20] C. M. Wilson, G. Johansson, A. Pourkabirian, M. Simoen, J. R. Johansson, T. Duty, F. Nori, and P. Delsing, Observation of the dynamical casimir effect in a superconducting circuit, *Nature (London)* **479**, 376 (2011).
- [21] P. D. Nation, J. R. Johansson, M. P. Blencowe, and F. Nori, *Colloquium*: Stimulating uncertainty: Amplifying the quantum vacuum with superconducting circuits, *Rev. Mod. Phys.* **84**, 1 (2012).
- [22] J. R. Johansson, G. Johansson, C. M. Wilson, P. Delsing, and F. Nori, Nonclassical microwave radiation from the dynamical casimir effect, *Phys. Rev. A* **87**, 043804 (2013).
- [23] X. Gu, A. F. Kockum, A. Miranowicz, Y. xi Liu, and F. Nori, Microwave photonics with superconducting quantum circuits, *Phys. Rep.* **718–719**, 1 (2017).
- [24] E. M. Purcell, H. C. Torrey, and R. V. Pound, Resonance absorption by nuclear magnetic moments in a solid, *Phys. Rev.* **69**, 37 (1946).
- [25] M. Tokman, Z. Long, S. AlMutairi, Y. Wang, M. Belkin, and A. Belyanin, Enhancement of the spontaneous emission in sub-wavelength quasi-two-dimensional waveguides and resonators, *Phys. Rev. A* **97**, 043801 (2018).
- [26] V. S. C. Manga Rao and S. Hughes, Single quantum-dot Purcell factor and β factor in a photonic crystal waveguide, *Phys. Rev. B* **75**, 205437 (2007).
- [27] R. Mitsch, C. Sayrin, B. Albrecht, P. Schneeweiss, and A. Rauschenbeutel, Quantum state-controlled directional spontaneous emission of photons into a nanophotonic waveguide, *Nat. Commun.* **5**, 5713 (2014).
- [28] I. Söllner, S. Mahmoodian, S. L. Hansen, L. Midolo, A. Javadi, G. Kiršanskė, T. Pregolato, H. El-Ella, E. H. Lee, J. D. Song, Søren Stobbe, and P. Lodahl, Deterministic photon–emitter coupling in chiral photonic circuits, *Nat. Nanotechnol.* **10**, 775 (2015).
- [29] K. Y. Bliokh, D. Smirnova, and F. Nori, Quantum spin Hall effect of light, *Science* **348**, 1448 (2015).
- [30] K. Y. Bliokh, D. Leykam, M. Lein, and F. Nori, Topological non-Hermitian origin of surface Maxwell waves, *Nat. Commun.* **10**, 580 (2019).
- [31] M. Maffei, D. Pomarico, P. Facchi, G. Magnifico, S. Pascazio, and F. V. Pepe, Directional emission and photon bunching from a qubit pair in waveguide, *Phys. Rev. Res.* **6**, L032017 (2024).
- [32] D. E. Chang, L. Jiang, A. V. Gorshkov, and H. J. Kimble, Cavity QED with atomic mirrors, *New J. Phys.* **14**, 063003 (2012).
- [33] M. Mirhosseini, E. Kim, X. Zhang, A. Sipahigil, P. B. Dieterle, A. J. Keller, A. Asenjo-Garcia, D. E. Chang, and O. Painter, Cavity quantum electrodynamics with atom-like mirrors, *Nature (London)* **569**, 692 (2019).

- [34] T. M. Karg, B. Gouraud, P. Treutlein, and K. Hammerer, Remote Hamiltonian interactions mediated by light, *Phys. Rev. A* **99**, 063829 (2019).
- [35] A. S. Sheremet, M. I. Petrov, I. V. Iorsh, A. V. Poshakinskiy, and A. N. Poddubny, Waveguide quantum electrodynamics: Collective radiance and photon-photon correlations, *Rev. Mod. Phys.* **95**, 015002 (2023).
- [36] S. Hughes, Coupled-cavity QED using planar photonic crystals, *Phys. Rev. Lett.* **98**, 083603 (2007).
- [37] D. Mukhopadhyay and G. S. Agarwal, Transparency in a chain of disparate quantum emitters strongly coupled to a waveguide, *Phys. Rev. A* **101**, 063814 (2020).
- [38] E. Rephaeli, J.-T. Shen, and S. Fan, Full inversion of a two-level atom with a single-photon pulse in one-dimensional geometries, *Phys. Rev. A* **82**, 033804 (2010).
- [39] L. Guo, A. F. Kockum, F. Marquardt, and G. Johansson, Oscillating bound states for a giant atom, *Phys. Rev. Res.* **2**, 043014 (2020).
- [40] L. Guo, A. Grimsmo, A. F. Kockum, M. Pletyukhov, and G. Johansson, Giant acoustic atom: A single quantum system with a deterministic time delay, *Phys. Rev. A* **95**, 053821 (2017).
- [41] C. W. Gardiner and M. J. Collett, Input and output in damped quantum systems: Quantum stochastic differential equations and the master equation, *Phys. Rev. A* **31**, 3761 (1985).
- [42] E. Rephaeli and S. Fan, Few-photon single-atom cavity QED with input-output formalism in Fock space, *IEEE J. Sel. Top. Quantum Electron.* **18**, 1754 (2012).
- [43] S. Fan, S. E. Kocabaş, and J.-T. Shen, Input-output formalism for few-photon transport in one-dimensional nanophotonic waveguides coupled to a qubit, *Phys. Rev. A* **82**, 063821 (2010).
- [44] A. Roulet and V. Scarani, Solving the scattering of n photons on a two-level atom without computation, *New J. Phys.* **18**, 093035 (2016).
- [45] Z. Liao, Y. Lu, and M. S. Zubairy, Multiphoton pulses interacting with multiple emitters in a one-dimensional waveguide, *Phys. Rev. A* **102**, 053702 (2020).
- [46] F. Dinc, Diagrammatic approach for analytical non-Markovian time evolution: Fermi's two-atom problem and causality in waveguide quantum electrodynamics, *Phys. Rev. A* **102**, 013727 (2020).
- [47] L. Zhou, Z. R. Gong, Y.-x. Liu, C. P. Sun, and F. Nori, Controllable scattering of a single photon inside a one-dimensional resonator waveguide, *Phys. Rev. Lett.* **101**, 100501 (2008).
- [48] L. Zhou, H. Dong, Y.-x. Liu, C. P. Sun, and F. Nori, Quantum supercavity with atomic mirrors, *Phys. Rev. A* **78**, 063827 (2008).
- [49] L. Zhou, S. Yang, Y.-x. Liu, C. P. Sun, and F. Nori, Quantum Zeno switch for single-photon coherent transport, *Phys. Rev. A* **80**, 062109 (2009).
- [50] J.-Q. Liao, Z. R. Gong, L. Zhou, Y.-x. Liu, C. P. Sun, and F. Nori, Controlling the transport of single photons by tuning the frequency of either one or two cavities in an array of coupled cavities, *Phys. Rev. A* **81**, 042304 (2010).
- [51] T. Caneva, M. T. Manzoni, T. Shi, J. S. Douglas, J. I. Cirac, and D. E. Chang, Quantum dynamics of propagating photons with strong interactions: A generalized input-output formalism, *New J. Phys.* **17**, 113001 (2015).
- [52] J. Zhang, Y.-x. Liu, R.-B. Wu, K. Jacobs, and F. Nori, Quantum feedback: Theory, experiments, and applications, *Phys. Rep.* **679**, 1 (2017).
- [53] S. Arranz Regidor, G. Crowder, H. Carmichael, and S. Hughes, Modeling quantum light-matter interactions in waveguide QED with retardation, nonlinear interactions, and a time-delayed feedback: Matrix product states versus a space-discretized waveguide model, *Phys. Rev. Res.* **3**, 023030 (2021).
- [54] G. Crowder, L. Ramunno, and S. Hughes, Quantum trajectory theory and simulations of nonlinear spectra and multiphoton effects in waveguide-QED systems with a time-delayed coherent feedback, *Phys. Rev. A* **106**, 013714 (2022).
- [55] K. Barkemeyer, A. Knorr, and A. Carmele, Heisenberg treatment of multiphoton pulses in waveguide QED with time-delayed feedback, *Phys. Rev. A* **106**, 023708 (2022).
- [56] H. Pichler and P. Zoller, Photonic circuits with time delays and quantum feedback, *Phys. Rev. Lett.* **116**, 093601 (2016).
- [57] G. Crowder, H. Carmichael, and S. Hughes, Quantum trajectory theory of few-photon cavity-QED systems with a time-delayed coherent feedback, *Phys. Rev. A* **101**, 023807 (2020).
- [58] A. Carmele, N. Nemet, V. Canela, and S. Parkins, Pronounced non-Markovian features in multiply excited, multiple emitter waveguide QED: Retardation induced anomalous population trapping, *Phys. Rev. Res.* **2**, 013238 (2020).
- [59] S. A. Regidor, A. Knorr, and S. Hughes, Dynamical spectra from one and two-photon Fock state pulses exciting a single chiral qubit in a waveguide, [arXiv:2410.03715](https://arxiv.org/abs/2410.03715).
- [60] S. A. Regidor, A. Knorr, and S. Hughes, Theory and simulations of few-photon Fock state pulses strongly interacting with a single qubit in a waveguide: Exact population dynamics and time-dependent spectra, *Phys. Rev. Res.* **7**, 023295 (2025).
- [61] M. Gross and S. Haroche, Superradiance: An essay on the theory of collective spontaneous emission, *Phys. Rep.* **93**, 301 (1982).
- [62] A. V. Andreev, V. I. Emelyanov, and Y. A. Il'inskiĭ, Collective spontaneous emission (Dicke superradiance), *Sov. Phys. Usp.* **23**, 493 (1980).
- [63] N. Shammah, N. Lambert, F. Nori, and S. De Liberato, Superradiance with local phase-breaking effects, *Phys. Rev. A* **96**, 023863 (2017).
- [64] N. Lambert, Y. Matsuzaki, K. Kakuyanagi, N. Ishida, S. Saito, and F. Nori, Superradiance with an ensemble of superconducting flux qubits, *Phys. Rev. B* **94**, 224510 (2016).
- [65] K. Sinha, P. Meystre, E. A. Goldschmidt, F. K. Fatemi, S. L. Rolston, and P. Solano, Non-Markovian collective emission from macroscopically separated emitters, *Phys. Rev. Lett.* **124**, 043603 (2020).
- [66] R. Orús, A practical introduction to tensor networks: Matrix product states and projected entangled pair states, *Ann. Phys. (N.Y.)* **349**, 117 (2014).
- [67] C. Yang, F. C. Binder, V. Narasimhachar, and M. Gu, Matrix product states for quantum stochastic modeling, *Phys. Rev. Lett.* **121**, 260602 (2018).
- [68] L. Vanderstraeten, *Tensor Network States and Effective Particles for Low-Dimensional Quantum Spin Systems* (Springer, Cham, 2017).
- [69] N. L. Naumann, S. M. Hein, M. Kraft, A. Knorr, and A. Carmele, Feedback control of photon statistics, in *Physics*

- and Simulation of Optoelectronic Devices XXV*, edited by B. Witzigmann, M. Osinski, and Y. Arakawa (International Society for Optics and Photonics, Bellingham, 2017), Vol. 10098, p. 100980N.
- [70] L. Droenner, N. L. Naumann, E. Schöll, A. Knorr, and A. Carmele, Quantum Pyragas control: Selective control of individual photon probabilities, *Phys. Rev. A* **99**, 023840 (2019).
 - [71] K. Vodenkova and H. Pichler, Continuous coherent quantum feedback with time delays: Tensor network solution, *Phys. Rev. X* **14**, 031043 (2024).
 - [72] K. Sinha, A. González-Tudela, Y. Lu, and P. Solano, Collective radiation from distant emitters, *Phys. Rev. A* **102**, 043718 (2020).
 - [73] F. Dinc and A. M. Brańczyk, Non-Markovian superradiance in a linear chain of up to 100 qubits, *Phys. Rev. Res.* **1**, 032042(R) (2019).
 - [74] W. Alvarez-Giron, P. Solano, K. Sinha, and P. Barberis-Blostein, Delay-induced spontaneous dark-state generation from two distant excited atoms, *Phys. Rev. Res.* **6**, 023213 (2024).
 - [75] L. Scarpelli, B. Lang, F. Masia, D. M. Beggs, E. A. Muljarov, A. B. Young, R. Oulton, M. Kamp, S. Höfling, C. Schneider, and W. Langbein, 99% beta factor and directional coupling of quantum dots to fast light in photonic crystal waveguides determined by spectral imaging, *Phys. Rev. B* **100**, 035311 (2019).
 - [76] A. Blais, A. L. Grimsmo, S. M. Girvin, and A. Wallraff, Circuit quantum electrodynamics, *Rev. Mod. Phys.* **93**, 025005 (2021).
 - [77] I. P. McCulloch, From density-matrix renormalization group to matrix product states, *J. Stat. Mech.* (2007) P10014.
 - [78] U. Schollwöck, The density-matrix renormalization group in the age of matrix product states, *Ann. Phys. (N.Y.)* **326**, 96 (2011).
 - [79] H. Pichler, S. Choi, P. Zoller, and M. D. Lukin, Universal photonic quantum computation via time-delayed feedback, *Proc. Natl. Acad. Sci. USA* **114**, 11362 (2017).
 - [80] L. J. Droenner, Out-of-equilibrium dynamics of open quantum many-body systems, Ph.D. thesis, Technischen Universität Berlin, 2019.
 - [81] C. Liedl, F. Tebbenjohanns, C. Bach, S. Pucher, A. Rauschenbeutel, and P. Schneeweiss, Observation of superradiant bursts in a cascaded quantum system, *Phys. Rev. X* **14**, 011020 (2024).